

# ISTITUTO NAZIONALE DI FISICA NUCLEARE

Sezione di Genova

---

INFN/TC-97/18  
30 Giugno 1997

P. Fabbriatore, R. Musenich, C. Priano:

**ELECTRICAL CHARACTERIZATIONS OF THE SUPERCONDUCTING BABAR  
SOLENOID CONDUCTORS**

*SIS-Pubblicazioni*  
*dei Laboratori Nazionali di Frascati*

**ELECTRICAL CHARACTERIZATIONS OF THE SUPERCONDUCTING BABAR SOLENOID CONDUCTORS**

P. Fabricatore, R. Musenich and C. Priano

INFN – Sezione di Genova, Via Dodecaneso 33, I-16146, Genova, Italy

**ABSTRACT**

The superconducting solenoid for BABAR experiment at PEP-II at SLAC is at present time under construction at ANSALDO Energia in Genova. The coil is wound with an aluminium-stabilised conductor, constructed with a co-extrusion technique by Europa Metalli in partial co-operation with INFN, ETH and ALCATEL SWISS CABLES. Six lengths of about 1.8 Km were produced. The present paper deals with the electrical characterisations of short samples cut from each length. Electrical joints between conductors were also characterised. The measurements were performed in the facility MaRiSA, using a transformer method to charge the samples. It was found that the conductors were well above the specifications, causing the coil to operate with a margin higher than the designed one.

## 1. - THE CONDUCTORS

The BABAR superconducting solenoid [1], is designed to generate a magnetic field of 1.5 Tesla in a bore of about 3 m. In order to have a field homogeneity of 3% in the large volume occupied by the drift chamber, the current density in the winding is graded: lower in the central region, higher at the sides. The current being fixed, the gradation is obtained by using two different conductors: a thicker conductor for the central region and a thinner one for the sides. Both the conductors are composed by 16 strand Rutherford type cable, stabilised by pure aluminium (see Fig.1).

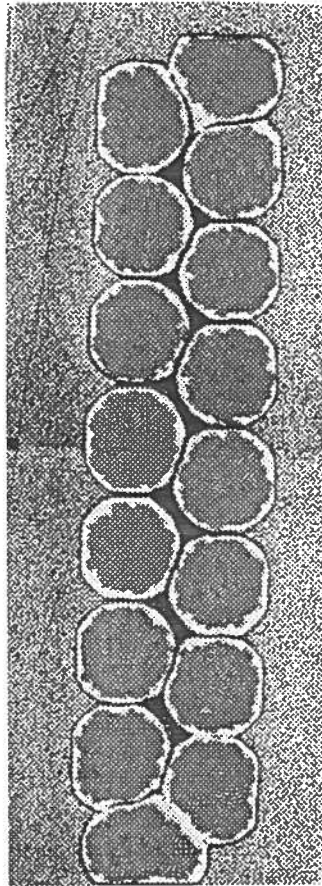


**Fig.1** Cross section of BABAR Rutherford cable immersed in the aluminium matrix.

Table I shows the strands, Rutherford and conductor characteristics as designed, while Table II summarises some characteristics of the produced conductors.

TABLE I – Summary of strands, Rutherford and conductor characteristics.

COMPONENT	CHARACTERISTIC	VALUE
<b>Strand</b>	NbTi	Nb 46.5 +/- 1.5 wt % Ti
	Filament size	< 40 $\mu$ m
	Twist pitch	25 mm
	Cu/NbTi ratio	> 1.1
	RRR	Final >100
	Wire diameter	0.8 mm $\pm$ 0.005
<b>Rutherford</b>	Transposition pitch	< 90 mm
	Number of strands	16
	Final size	1.4 x 6.4 mm <sup>2</sup>
<b>Conductor</b>	Al-RRR	>1000
	Dimensions: Thin conductor	(4.93 x 20) $\pm$ 0.02 mm
	Thick conductor	(8.49 x 20) $\pm$ 0.02 mm
	Rutherford-Al bonding	> 20 MPa
	Al/Cu/NbTi ratio: Thin conductor	23.5:1.1:1
	Thick conductor	42.4:1.1:1
	Edge curvature radius	> 0.2 mm
Critical current @ T=4.2 K; B=2.5 T	12680 A	

TABLE – II Characteristics of produced conductors.

Length # and type	Total produced length (m)	Average Rutherford dimensions (mm <sup>2</sup> )	Average conductor dimensions (mm <sup>2</sup> )	RRR
#1 thin	1959	(6.45 $\pm$ 0.01 x 1.45 $\pm$ 0.01)	(20.04 $\pm$ 0.02 x 4.975 $\pm$ 0.025)	1505
#3 thick	1651	(6.45 $\pm$ 0.01 x 1.45 $\pm$ 0.01)	(19.89 $\pm$ 0.03 x 8.40 $\pm$ 0.025)	1522
#4 thin	1870	(6.45 $\pm$ 0.01 x 1.45 $\pm$ 0.01)	(20.01 $\pm$ 0.03 x 5.00 $\pm$ 0.02)	1575
#5 thin	1905	(6.44 $\pm$ 0.01 x 1.47 $\pm$ 0.03)	(20.06 $\pm$ 0.02 x 4.975 $\pm$ 0.015)	1442
#7 thick	1853	(6.45 $\pm$ 0.01 x 1.45 $\pm$ 0.01)	(19.925 $\pm$ 0.025 x 8.425 $\pm$ 0.025)	1486
#9 thin	1894	(6.45 $\pm$ 0.01 x 1.45 $\pm$ 0.01)	(20.05 $\pm$ 0.03 x 5.025 $\pm$ 0.015)	1503

## 2 – MEASUREMENTS AND METHODS

Two different tests were performed on the short samples: critical current and joint resistance as function of magnetic field at 4.2 K. The tests will be performed using the MaRiSA test facility in the 6 T configuration and are based on the direct transformer method [2,3]. The basic electrical scheme is shown in Fig.2:

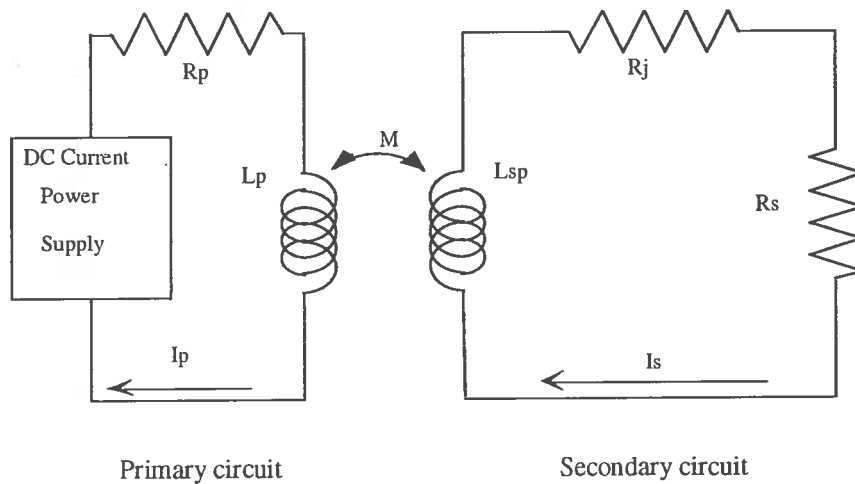


Fig. 2 Basic scheme of the transformer method.

The primary winding is the 6T MaRiSA magnet and the secondary winding is the sample itself arranged as a single loop of external radius  $R_e=201$  mm with a low resistance joint. The current transformer ratio is about 700.

### 2.1 – Critical Current

The current flowing in the sample is measured using 2 Hall probes, arranged as shown in Fig.3. The probe HP1 senses only the self-field generated by the current in the sample whilst the second probe HP2 is placed at the centre of the sample so that it senses both the field and the self-field.

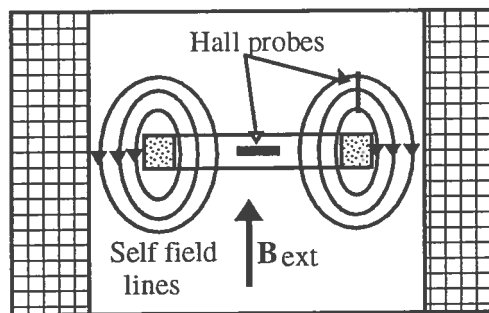


Fig.3 Layout for current measurements using two Hall Probes.

The HP2 probe is used for calibration: the field generated by a current flowing in the sample is few depending on the position at the magnetic centre, so that, on inducing a current in the sample at a low level of the applied field (1000-2000 Gauss) it is possible to measure with good accuracy (less than 0.5 %) the self field. A comparison between measured and calculated self fields, which is of the order of 300 Gauss at a current of 10KA, gives the current in the sample. During the same calibration procedure the signal at the HP1 probe can be related to the current in the sample. At high field ( $B > 1T$ ), the signal at HP2 is mainly given by the applied field so that only the signal at HP1 can be used, as this signal is mainly determined by the self-field. Nevertheless it is not possible to neglect at all the background magnetic field at HP1, so that the current measurements are affected by a bias signal depending on the background magnetic field strength. Due to variations of the background field detected by the HP1 probe, caused by small movements of the sample, the accuracy of measurement is 2-3%.

The critical current measurement is performed according to the following steps:

- 1- The background magnetic field is set to a given value  $B_i$  then the sample is kept in normal state by turning on the heater so that any induced current is removed in the loop.
- 2- The field is ramped down and the voltage  $V_M$  at the voltage taps is monitored versus the current in the sample given by the HP1 signal.
- 3- When the voltage  $V_M$  increases due to a transition, the field ramp is stopped at a value  $B_F$  and the current decays slowly according to the circuit time constant (200 - 1500 s):

$$\tau = \frac{L_{loop}}{R_j + R_S}, \quad (1)$$

allowing to record the V-I characteristics (see Fig.4).

- 5- The critical current is defined by the resistive criterion  $10^{-14} \Omega \cdot m$ . The measurement external field is  $B_F$  and  $T=4.2$  K (the sample is immersed in a liquid helium bath).

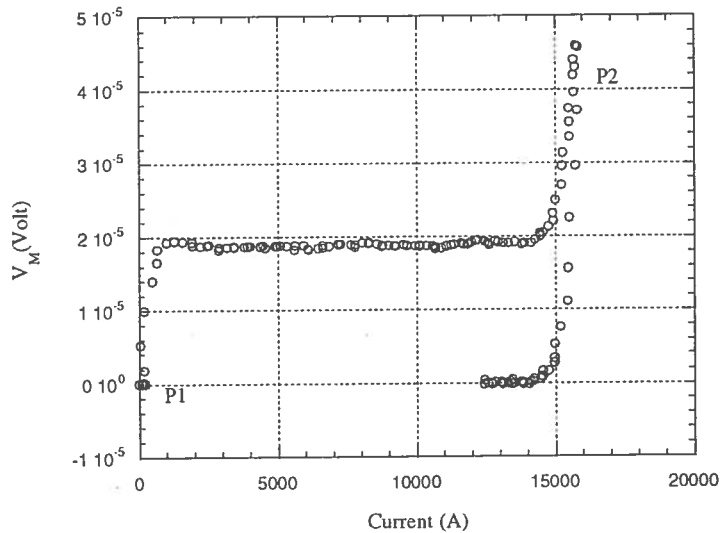


Fig.4 I-V characteristic monitored during a typical inductive critical current measurements. At P1 starts the external field ramp down, while at P2 the ramp is stopped and the current decay is started.

## 2.2 – Joint Resistance

When constructing the magnet, joints inevitably occur between two different lengths. The joint resistance measurement is performed using the current decay method (CD). The sample is arranged in the layout showed in Fig.3 and the measurement is performed according to the following steps:

- 1- The background magnetic field is set to a given value  $B_i$  and the sample is kept in normal state by turning on the heater.
- 2- The field is ramped down to a pre-set value  $B_f$  and a current is induced in the superconducting loop.
- 3- The current decays slowly allowing to record the self field (HP1 probe signal) Vs the time (Fig.5). For  $I < I_c$  the circuit time constant is:

$$\tau = \frac{L_{loop}}{R_j} \quad (2)$$

where  $L_{loop}$  is the inductance of the sample and  $R_j$  is the joint resistance.

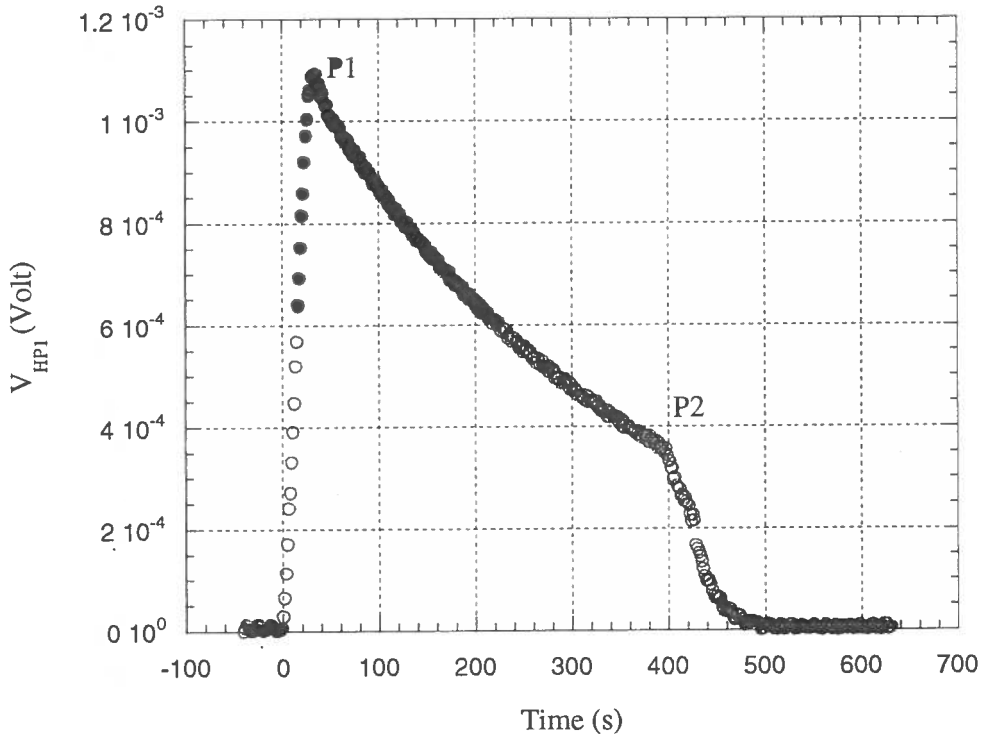


Fig.5 CD signal monitored for hall probe HP1. At P1 the ramp field is stopped and starts the CD, at P2 the sample is heated to remove any residual current from the loop.

By fitting the experimental data from P1 to P2 with an exponential law we obtain the time constant of the loop. The loop inductance  $L_{loop}$  being obtained by computation, the joint resistance is determined dividing  $L_{loop}$  by the time constant.

### 3 – SAMPLE PREPARATIONS, MEASUREMENT RESULTS

The critical current measurements are carried out on the Rutherford cables extracted from pure aluminium matrix by a chemical etching. The sample is arranged with the field normal to the wide face in order to reproduce the same field configuration of the conductor inside the winding. Due to the limitations in dimension of the MaRiSA bore (440 mm), it is not possible to bend directly the Al-stabilised conductor on the higher inertia. The Rutherford cable must be adequately supported to avoid any movements due to the magnetic force. A reliable support to the conductor can be obtained by soft solder it into a seat made on a copper ring as shown in Fig.6. The joint is made by overlapping the conductor ends for at least a twist pitch.

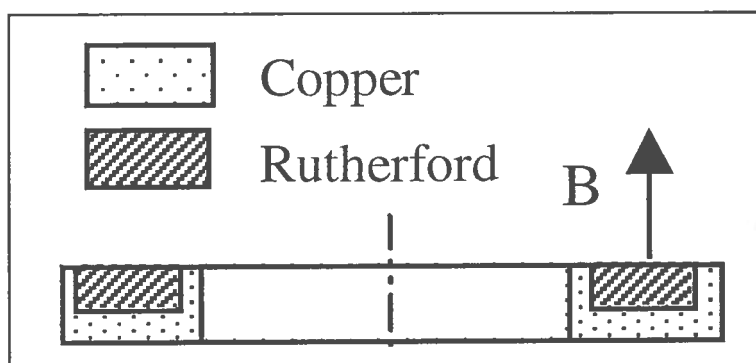


Fig.6 Sample holder layout for the critical current measurements.

For each length critical current measurements were performed on short samples at different magnetic field (Fig.7) and a value was extrapolated at the magnetic field of 2.5 T (Table III) in order to compare it with the specification one:  $I_c(B=2.5 \text{ T}; T=4.2 \text{ K})=12680 \text{ A}$ .

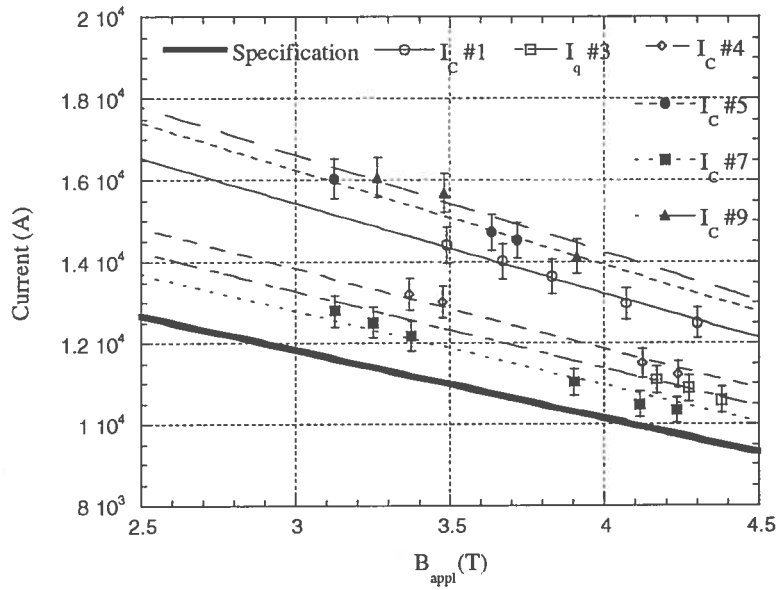
In sample #3 the transition showed in Fig.4 was not observed, because the sample quenches before to measure a significant voltage. This occurs some times when the sample is not properly soldered inside the sample holder. Then for this sample only the quench current, at different applied magnetic field, was measured. Though those values are lower than the real critical currents, they are higher than those ones required by the critical current specifications (see Fig.7), allowing to consider the sample inside the specifications.

TABLE – III Results of the critical current tests.

Sample	Co-extruded on	Tested on	$I_c$ ( $B=2.5 \text{ T}, T=4.2\text{K}$ )	N value
#1	30-10-1996	19-11-1996	16800 A	27
#3	29-10-1996	11-12-1996	15430 A*	//
#4	16-01-1997	19-02-1997	15250 A	29
#5	16-01-1997	10-02-1997	17660 A	40
#7	20-02-1997	5-03-1997	14250 A	20
#9	1-04-1997	9-05-1997	17810 A	36

\* This value refers to the quench current.





**Fig.7** Critical current and quench currents Vs applied field (were for applied filed we mean the external field plus the sample self field ( $B_{sf}=0.68$  Gauss/A)) performed on the six samples. The thick solid line represents the specification.

The joint measurements are carried out on the aluminium-stabilised conductor. The conductor joints, inside the magnet, are made by superimposing the two ends for a 1.5 m length and by TIG welding the pure aluminium. The joint tests are performed on 0.15 m long joints, i.e. about two twist pitch, so that the resistance of the full length joint can be obtained by linear extrapolation. The full conductor is bent on the lower inertia, so that the field is parallel to the wide face (Fig.8). Though the conductor in the winding experiences a different field orientation, this measurement is not required to be so accurate as a critical current test. In this case it is only necessary to have a rough idea about the used joint technology.

Two joints were measured on samples cut by length #1 and #7. In Fig.9 the joint resistivity at different fields are plotted, while in Table IV the values extrapolated at  $B=2.5$  T are reported.

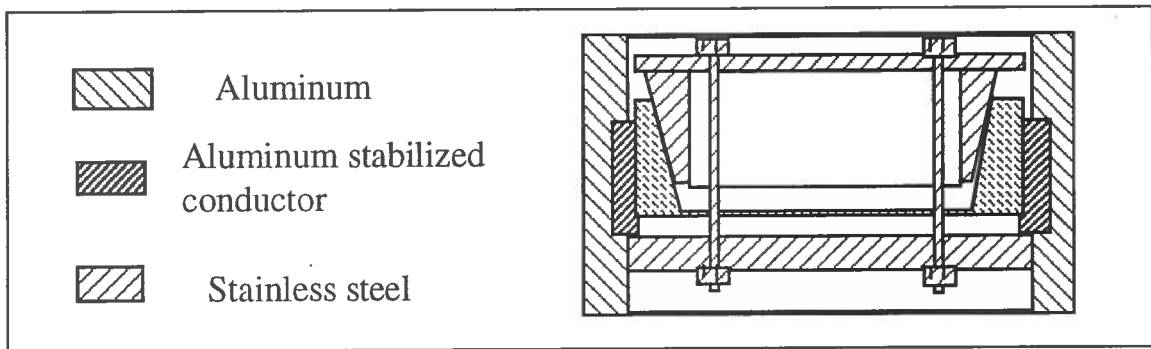


**Fig.8** Sample holder layout for the joint resistance measurements.

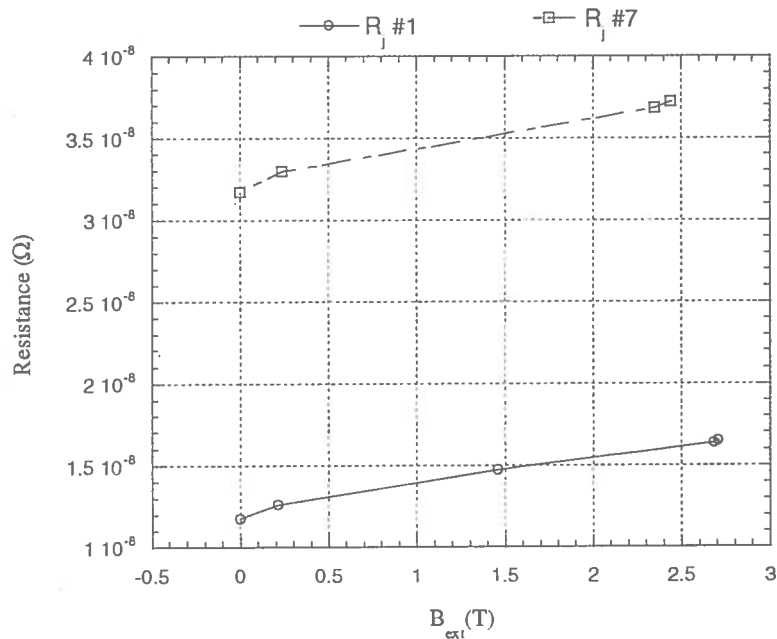


Fig.9 Joint resistance measurements Vs the external field.

TABLE – IV Joint resistance values extrapolated at  $B_{ext}=2.5$  T.

Sample	Joint Resistance ( $\Omega$ )	Joint Resistance per meter
#1	$1.62 \cdot 10^{-8}$	$2.43 \cdot 10^{-9}$
#7	$3.72 \cdot 10^{-8}$	$5.58 \cdot 10^{-9}$

From the values of Table IV we can calculate the heat dissipated by the joint inside the magnet at the operating current (about 5000 A). The joint inside the winding are about 1.5 m length and hence we found a dissipated heat  $H=0.0405$  W for joint #1 and  $H=0.093$  W for joint #7. This heat can be easily removed by the cooling system. However the real joint includes also a soft soldered part, so that the real dissipation should be much lower (in FINUDA coil  $R_{joint} \approx 5 \cdot 10^{-10} \Omega$ ).

#### 4 - MARGINS

In this section we will discuss the margins in terms of operating temperature with respect critical temperature and enthalpy reserve. Before giving details, we recall some basic relations [4].

The critical temperature with no current flowing in the conductor,  $T_c$ , only depends on the magnetic field. For NbTi the critical temperature depends on field according to

$$T_c(B) = T_{c0} \left(1 - \frac{B}{B_{c20}}\right)^{0.59} \quad (3)$$

where  $T_{c0}$  is the critical temperature at  $B = 0$  ( $T_{c0} = 9.3$  K) and  $B_{c20}$  is the critical field at  $T_c = 0$  ( $B_{c20} = 13.9$  T). The peak field in BABAR winding according to the preliminary design (with 1 layer coil) was  $B_{\text{peak}} = 2.5$  T. Using Eq.3 the critical temperature is  $T_c = 8.27$  K. Considering that a current  $I_0$  flows in the conductor, a new critical temperature  $T_g$  is defined, as the maximum temperature for which the current  $I_0$  can flow, with no dissipation, in the superconducting part.  $T_g$  is the important critical parameter and it is called current sharing temperature.

$$T_g = T_c - (T_c - T_0) \frac{I_0}{I_c(T_0, B)} \quad (4)$$

where  $I_c(T_0, B)$  is the critical current at nominal temperature and peak field. Since  $T_0 = 4.5$  K,  $B = 2.5$  T, the design current  $I_0 = 4600$  A and, from specification issued by ANSALDO,  $I_c @ 2.5$  T and 4.5 K is 11730 A, we have  $T_g = 6.79$  K.

During the engineering design the coil configuration was modified from 1 layer to 2 layers. This led to a reduction of the peak field at the thin conductor from 2.5 T to 2.3 T. The peak field at the thick conductor was calculated to be 1.6 T.

After completion of the winding the expected nominal current  $I_n$  is slightly higher than the designed one because the packing factor was lower:  $I_n = 4650$  A

We can now calculate again the margins, considering these modifications of the important parameters (Peak field, Critical current, Nominal current). The results are shown in Table V for the three sectors of the inner layer (the most critical ones).

Table V: Electrical and thermal margins of BABAR coil as constructed.

Length	$B_{\text{peak}}$ (T)	$I_c$ (A) $T=4.5$ K, $B=B_{\text{peak}}$	$I_n/I_c$	$T_g$ (K)
#5 inner layer thin forward	2.3	16550	28%	7.28
#7 inner layer thick middle	1.6	14220	33%	7.30
#9 inner layer thin backward	2.3	16950	27%	7.30

The resulted coil has more margin than the designed coil. In fact it is possible to tolerate an increase of temperature up to 2.68 K higher than the nominal one. A parameter of interest is the enthalpy variation from 4.5 K to 7.28 K:

$$E_{u.v.} = \int_{4.5}^{7.25} C_p(T) \delta dT \quad (5)$$

where  $C_p(T)$  is the specific heat (in J/Kg) and  $\delta$  the density. By averaging the thermal properties among the four parts of the winding (Aluminium, Copper, NbTi and fiberglass epoxy), we find  $E_{u.v.}=3635 \text{ J/m}^3$ . This enthalpy margin can be re-written in a more convenient way as energy per unit conductor length, resulting  $E_{u.l.} = 0.36 \text{ J/m}$  for thin conductor and  $E_{u.l.} = 0.65 \text{ J/m}$  for thick conductor. As comparison, two well know running magnets as ALEPH and CDF have  $E_{u.l.}$  respectively  $0.35 \text{ J/m}$  and  $0.1 \text{ J/m}$ .

The main conclusion of this paper is that according to the critical current measurements on short samples the BABAR coil results having higher margin than designed. The enthalpy margin is as high as a very large coil like ALEPH. This would lead to more safety operation of the coil, minimising the risks of premature quenching due to disturbances or wrong operation (lack of coolant, too fast charge and dis-charge).

## ACKNOWLEDGEMENTS

We wish to thank Mr Thomas O'Connor for having provided us the conductor micrography.

## REFERENCES

- 1 "The superconducting magnet for the BABAR detector of the PEP-II B factory at SLAC"  
P. Fabbriatore, E. Baynham, T. G. O'Connor, R.A. Bell et all  
IEEE Trans. On Magn., 1996 Vol 32, No 4, p. 2210
- 2 "Problemi connessi alle misure di corrente critica di conduttori ad alta corrente"  
P.Fabbriatore, R.Musenich and R. Parodi  
INFN/TC-92/06,1992
- 3 "Critical current measurements on the cables for LHC detector magnets"  
P.Fabbriatore, R.Musenich, R. Parodi and G:Gemme  
Presented at the 14<sup>th</sup> International Conference on Magnet Technology, Tampere June 1995
- 4 "Superconducting Magnets"  
M. N. Wilson  
Clarendon Press, Oxford, 1983